CHAPTER V

WIRELINE FORMATION TEST IN SINGLE LAYER HOMOGENEOUS RESERVOIR

The first simulation run is a base case which is a single layer homogeneous reservoir with oil as fluid formation. This simulation was performed in order to confirm the accuracy of the numerical solution with the analytical solution. In this chapter, the simulator was used to generate a number of cases in order to investigate the effects of probe size and effects of permeability anisotropy and to compare the results of Pressure Transient Analysis (PTA) technique with the simulation input data.

5.1 Base Case

A "Base Case" is chosen as a reference example for the simulation of mud filtrate invasion. Additionally, the base case is used to confirm the accuracy of the model set-up. The radial and theta permeability is 10 mD with permeability anisotropy (K_z/K_{xy}) of 0.1. Therefore, the vertical permeability is equal to 1 mD. Fluid drawdown test takes place for 30 minutes with a flow rate of 0.8 stb/day, followed by a shut-in or buildup test for 90 minutes. In fact, the testing period of an actual wireline formation test is very small but in our theoretical model a longer period was used in order to define all possible flow regimes such as radial flow. A schematic reservoir description for the base case is shown in Figure 5.1.

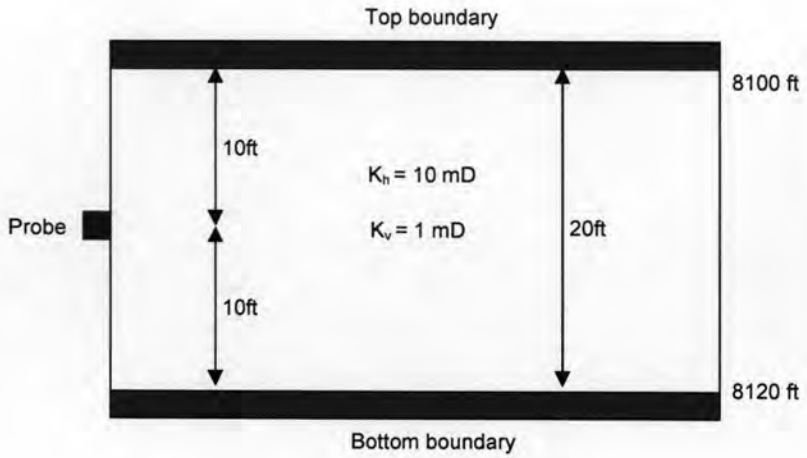

Figure 5.1 : Schematic reservoir description for the base case.

From the reservoir simulation run, the pressure response during drawdown and buildup test of the base case is shown in Figure 5.2. After that, the simulation result can be interpreted by using interpretation software as shown in Figures 5.3 and 5.4. In this study, we use two different interpretation programs which are Weltest200 and Saphir. Figure 5.3 depicts the diagnostic plot from Weltest200. The spherical flow model can be matched with the data at time between 0.01 hr to 0.1 hr, and the vertical to horizontal permeability, k_z/k_{xy}, can be estimated. At late time, after 0.2 hr, the radial flow model can also be matched to the data and the horizontal permeability, k_{xy}, can be estimated. Figure 5.4 depicts a regression fit to the test from Saphir interpretation program by using vertical interference model option in the software. We have adjusted some function in the vertical interference model to substitute for single probe wireline formation test in single well model. The regression shows a good match on the log-log diagnostic plot. From the regression, the reservoir parameters can be estimated. Table 5.1 is a comparison between estimated values from interpretation program and the value used to input into the reservoir simulation. The comparison shows that the estimates of parameters obtained from interpreting the pressure response from simulated wireline formation test are consistent with the input used in simulating the wireline formation test.

Table 5.1 : Comparison between input parameters and estimates from test interpretation.

Parameter	Input (mD)	Interpreted result (mD)	Error (%)
K_{xy}	10	9.931	-0.69
K_z	1	0.895	-10.5
K_{xyz}	4.642	4.452	-4.09
K_z/K_{xy}	0.1	0.09012	-9.88

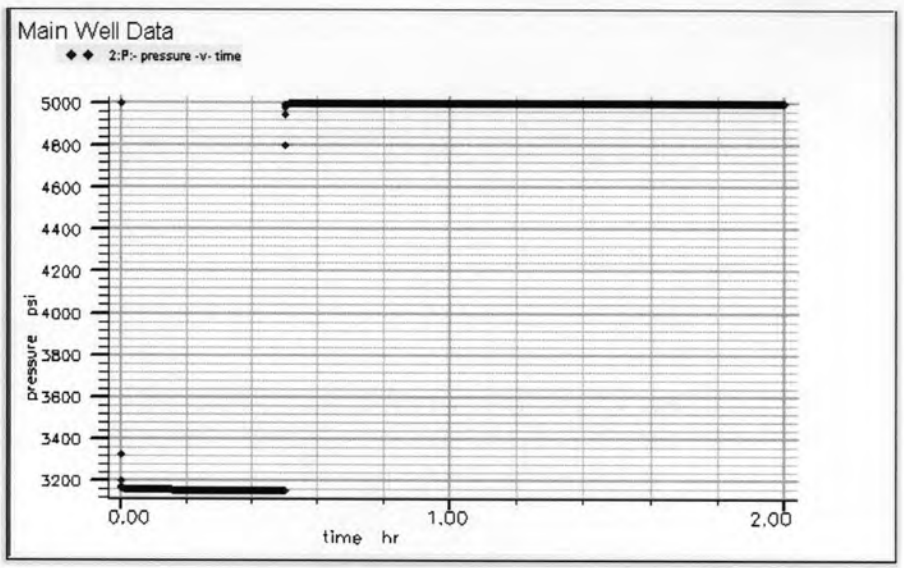

Figure 5.2 : Pressure history of the base case.

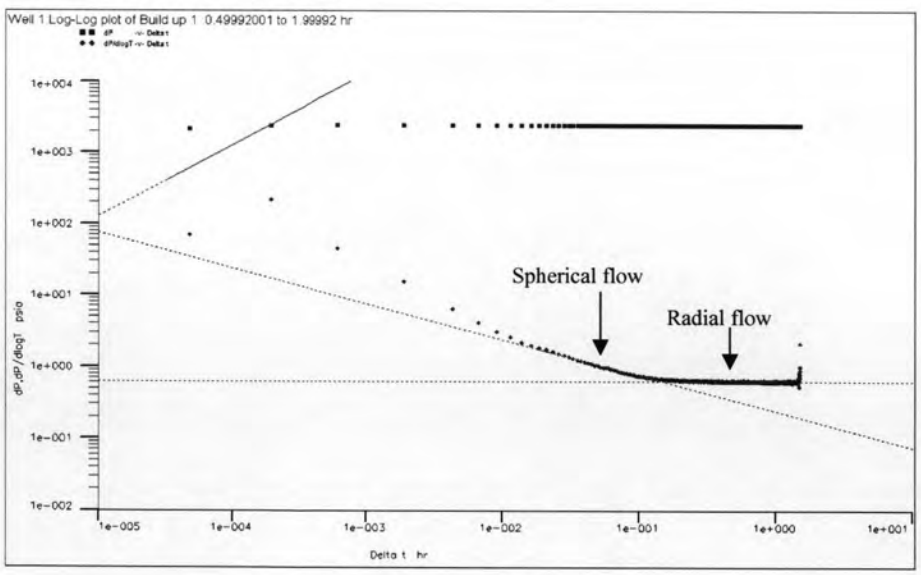

Figure 5.3 : Diagnostic plot for the base case.

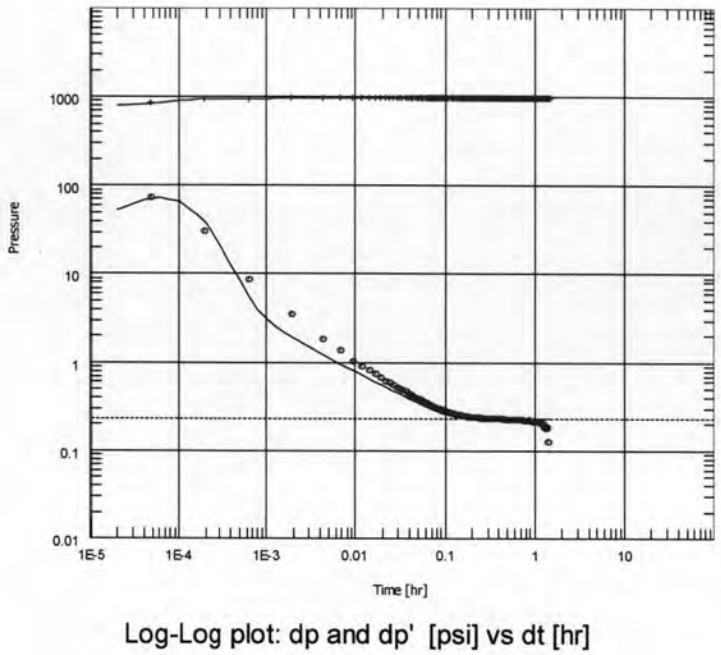

Figure 5.4 : Regression plot for the base case.

5.2 Effects of Probe Size

In this case study, the objective is to investigate the effects of probe size on pressure transients by varying probe size from case to case. Three different probe sizes which are 0.15, 0.85, and 2.16 square inch represent the cross sectional area of standard, large, and extra-large probe, respectively. The radial and theta permeabilities are fixed at 10 mD, and the vertical permeability is set at 1 mD. The schematic of reservoir model is shown in Figure 5.5. The flow rate is set to be 0.4 stb/d. The flow period consists of a 30-minute drawdown and a 90-minute buildup. After obtaining the pressure from reservoir simulation, the pressure response was then interpreted by graphical techniques. The pressure history and the diagnostic plots of the tests are shown in Figures 5.6 and 5.7, respectively, and the interpreted results are tabulated in Table 5.2. Figure 5.8 represents regression fits to the tests.

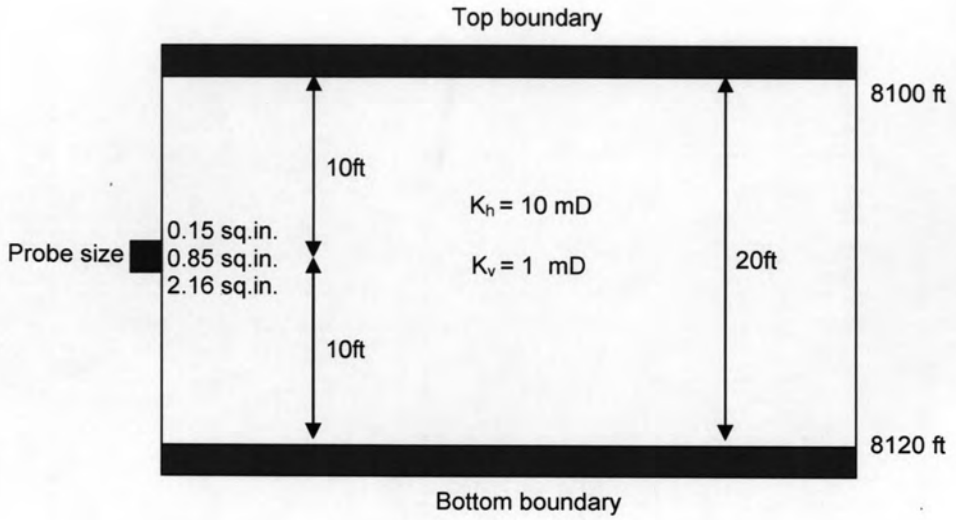

Figure 5.5 : Schematic reservoir description with different probe sizes.

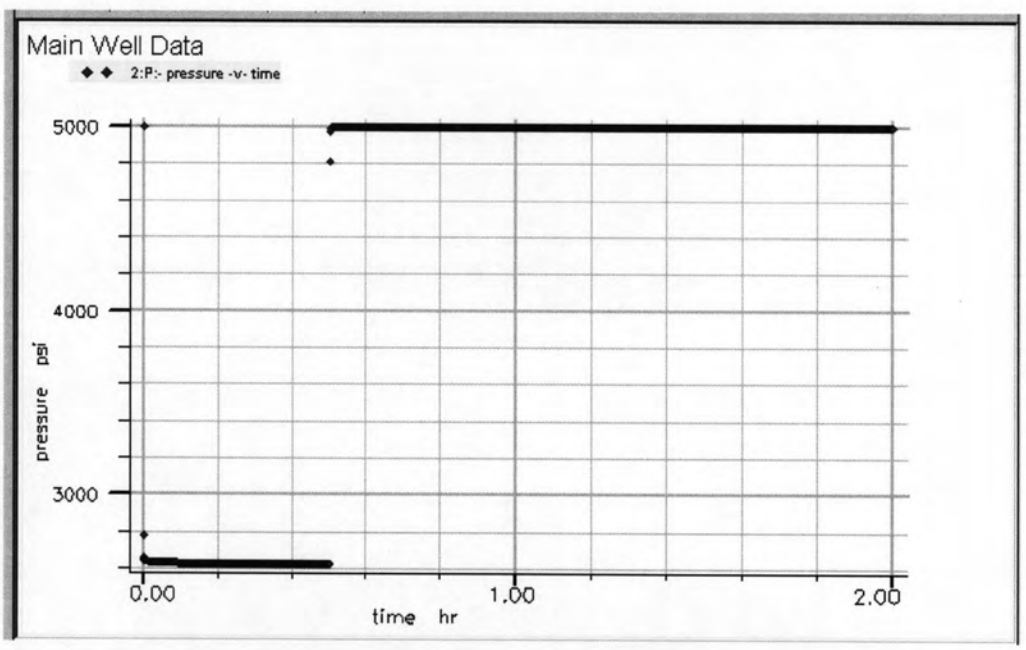

(a) Standard probe size case.

Figure 5.6 : Pressure history for different probe sizes.

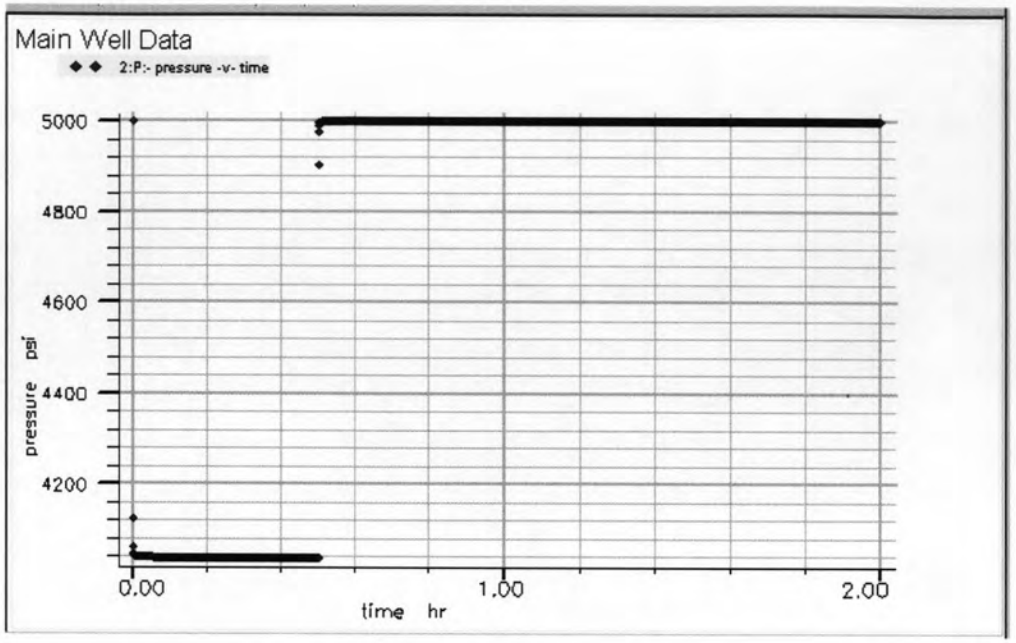

(b) Large probe size case.

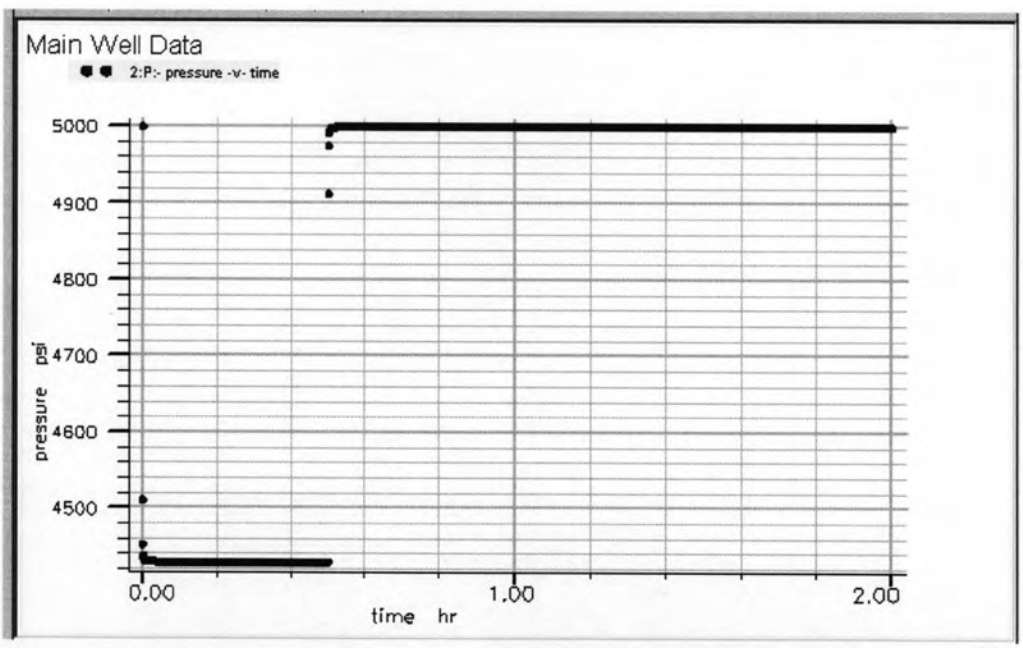

(c) Extra-large probe size case.

Figure 5.6 : Pressure history for different probe sizes (continued).

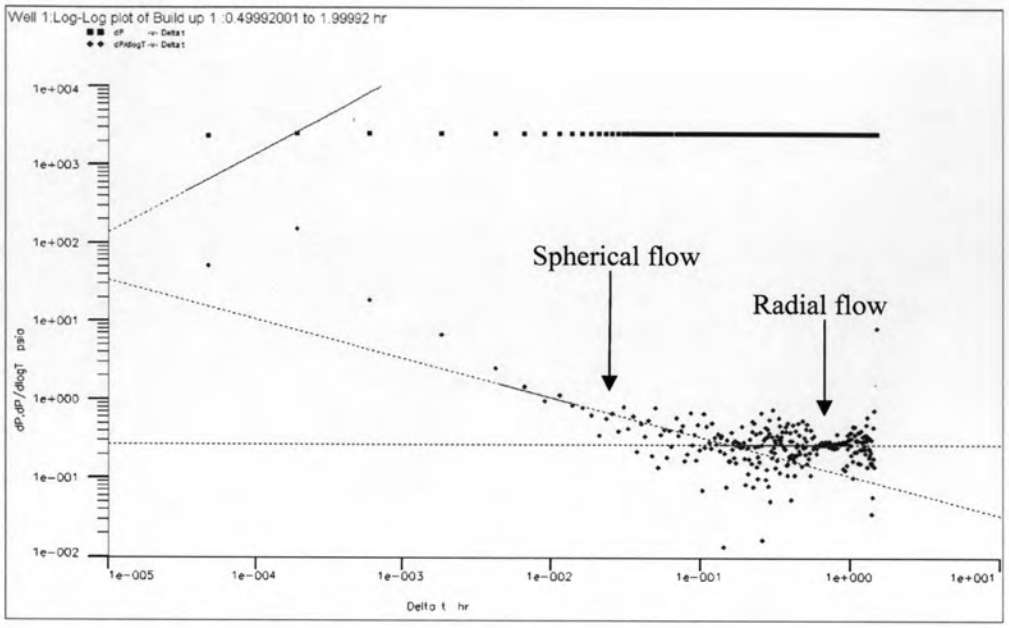

(a) Standard probe size case.

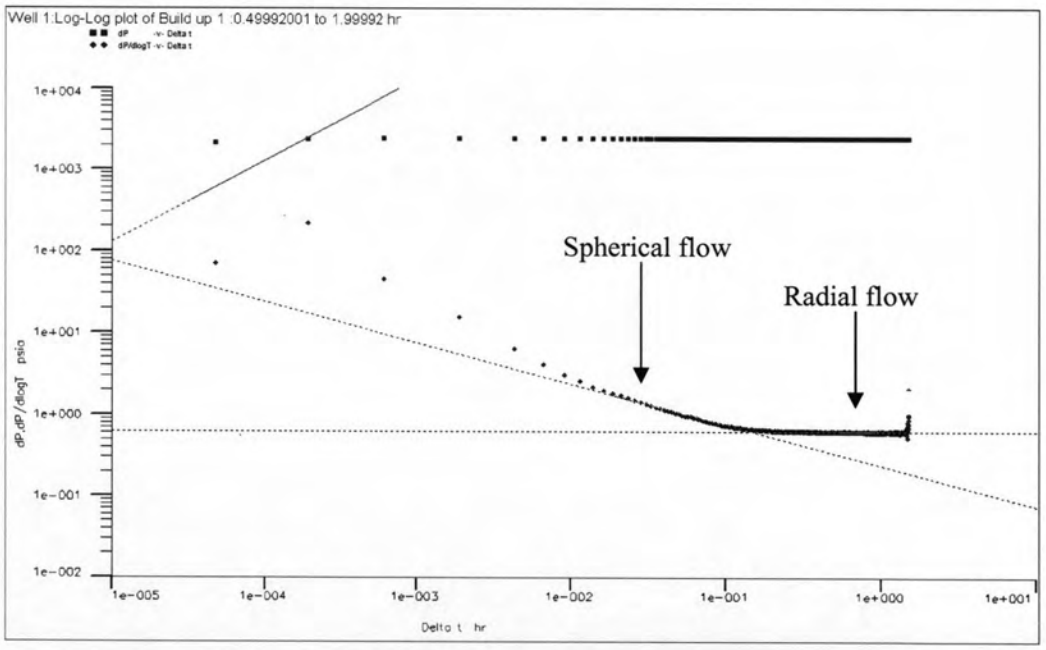

(b) Large probe size case.

Figure 5.7 : Diagnostic plots for different probe sizes.

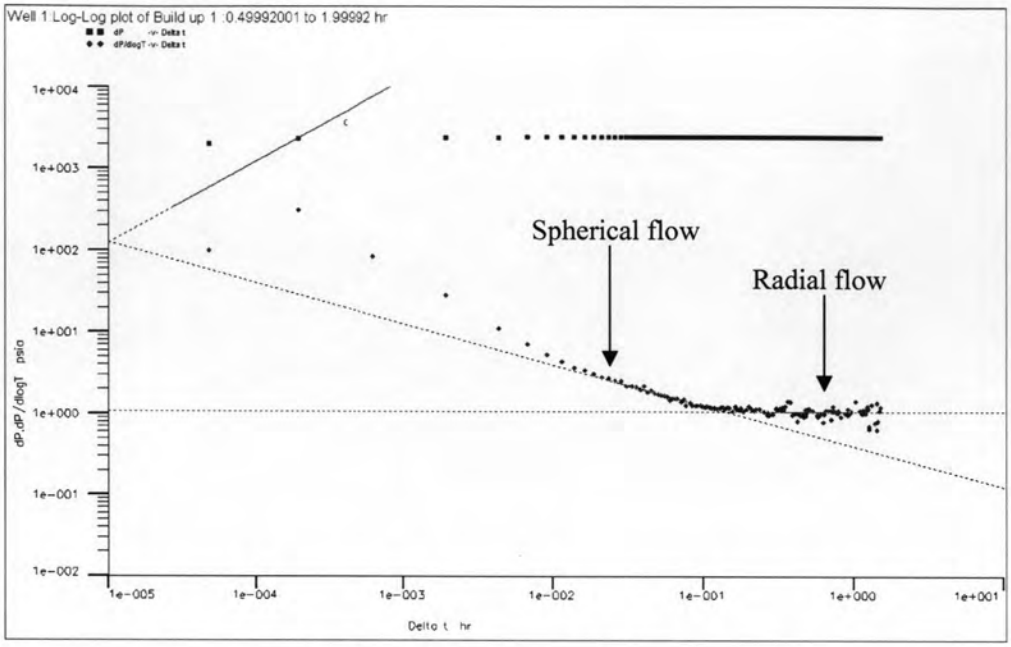

(c) Extra-large probe size case.

Figure 5.7 : Diagnostic plots for different probe sizes (continued).

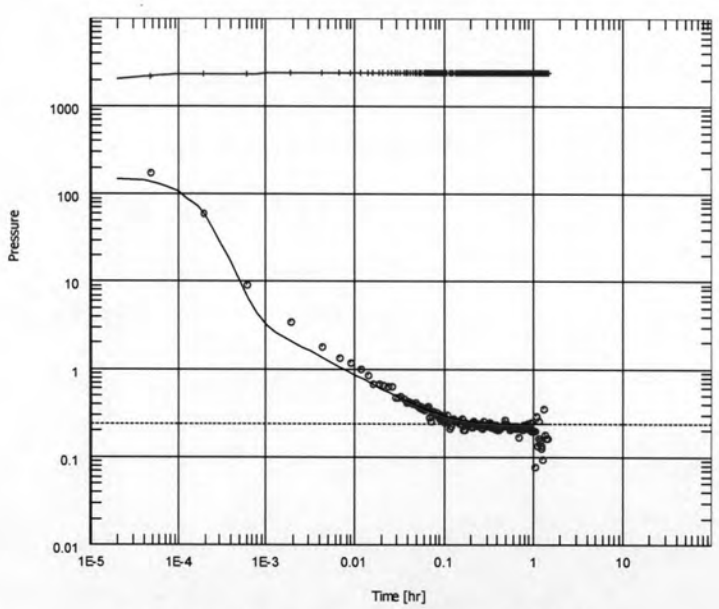

Log-Log plot: dp and dp' [psi] vs dt [hr]

(a) Standard probe size case.

Figure 5.8 : Regression plots for different probe sizes.

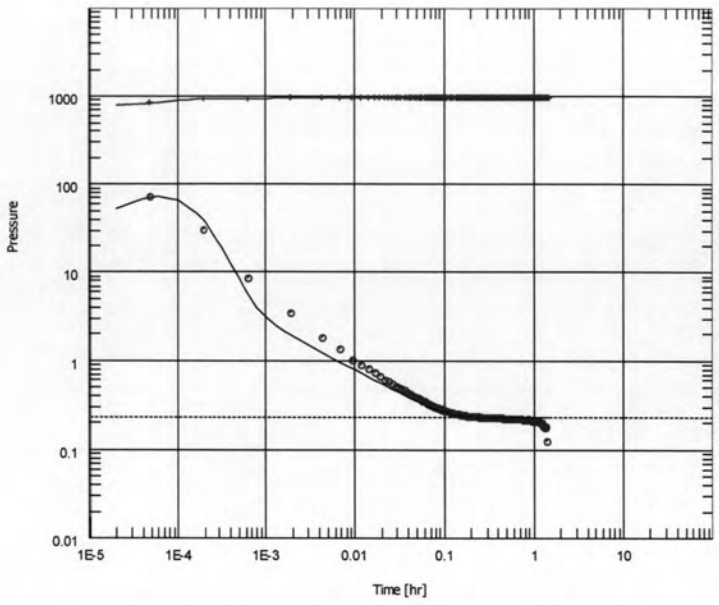

(b) Large probe size case.

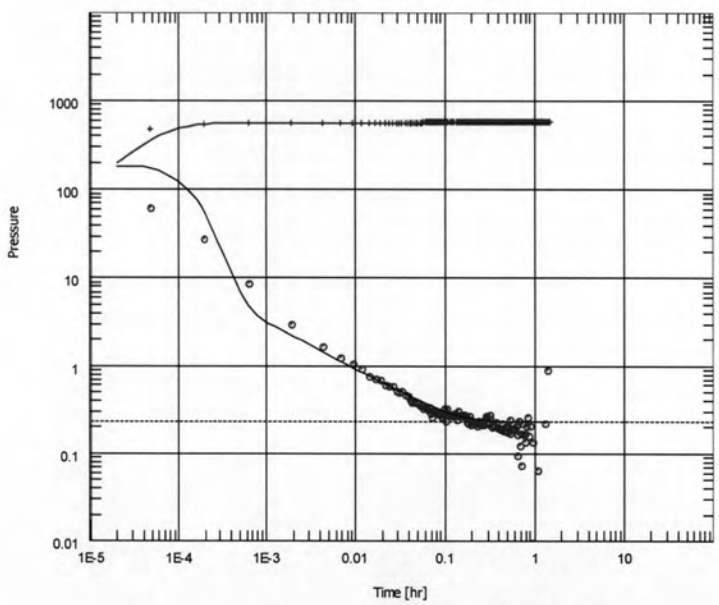

(c) Extra-large probe size case.

Figure 5.8 : Regression plots for different probe sizes (continued).

Table 5.2 : Interpreted results of different probe sizes.

Case	Probe size (sq.in.)	Interpreted results		Error (%)	
		Kxy	Kz	Kxy	Kz
Standard	0.15	8.784	0.604	-12.16	-39.6
Large	0.85	9.931	0.895	-0.69	-10.5
Extra-large	2.16	9.876	0.908	-1.24	-9.2

As can be seen in Figure 5.7 (a), (b), and (c), the spherical flow model can be matched with the data at time between 0.01 hr to 0.1 hr. At late time, after 0.2 hr, the radial flow model can be matched with the data. Both spherical flow and radial flow model regimes are well matched in the case of large and extralarge probe as depicted in Figure 5.8 (a), (b), and (c).

For the standard probe, as shown in Figure 5.7 (a), the pressure derivative in the diagnostic plot is more scattered than that of the large probe, shown in Figure 5.7 (b), and that of the extra-large probe, shown in Figure 5.7 (c). Since the size of standard probe is too small compared to the default minimum pore volume or keyword MINPV in the reservoir simulator, we have to adjust the value of MINPV otherwise the case cannot be run. The numerical errors of standard probe might be caused by this adjustment.

For extra-large probe, as shown in Figure 5.7 (c), there are some noise on the diagnostic plot because the simulated pressure drop is less than that of large probe size as shown in Figure 5.6 (c) and (a), respectively.

The interpreted results described in Table 5.2 indicate that the estimated error of K_{xy} of large probe case is less than other cases owing to smallest numerical error from reservoir simulation.

5.3 Effects of Permeability Anisotropy

In this case study, the objective is to investigate the effects of permeability anisotropy on pressure transients by keeping the same value of horizontal permeability but varying the vertical permeability from case to case. Five different permeability anisotropy ratios which are K_v/K_h of 0.01, 0.05, 0.1, 0.5, and 1 are considered. The radial and theta permeabilities are fixed at 10 mD while the vertical permeability varies with permeability anisotropy ratio as shown in Figure 5.9. The flow period consists of a 30-minute drawdown and a 90-minute buildup. After obtaining the pressure from reservoir simulations, the pressure response was then interpreted by graphical techniques. The diagnostic plots of the tests are shown in Figure 5.10, and the interpreted results are tabulated in Table 5.3. Figure 5.11 represents regression fits of the tests.

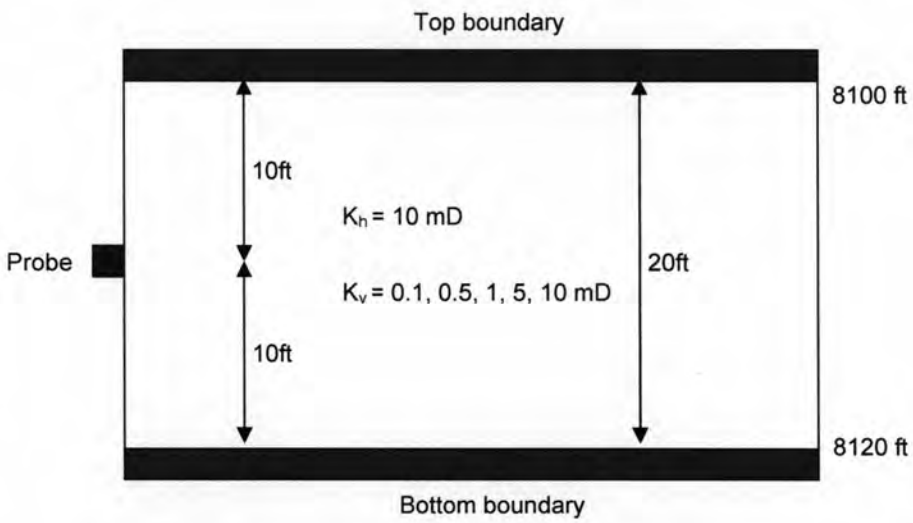

Figure 5.9: Schematic reservoir description with different permeability anisotropy ratios.

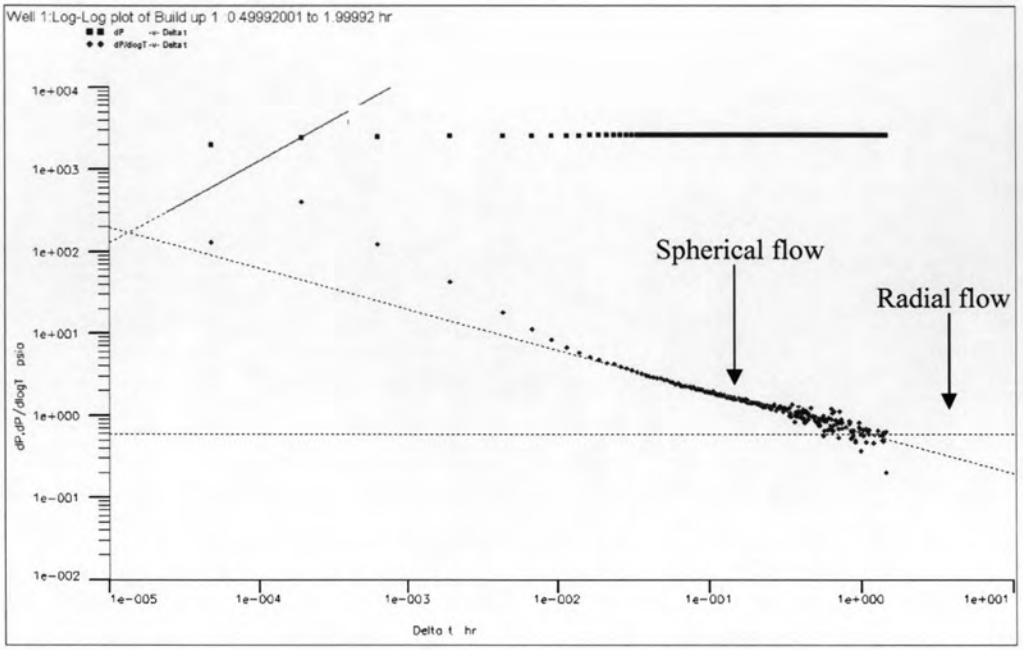

(a) Permeability anisotropy ratio of 0.01

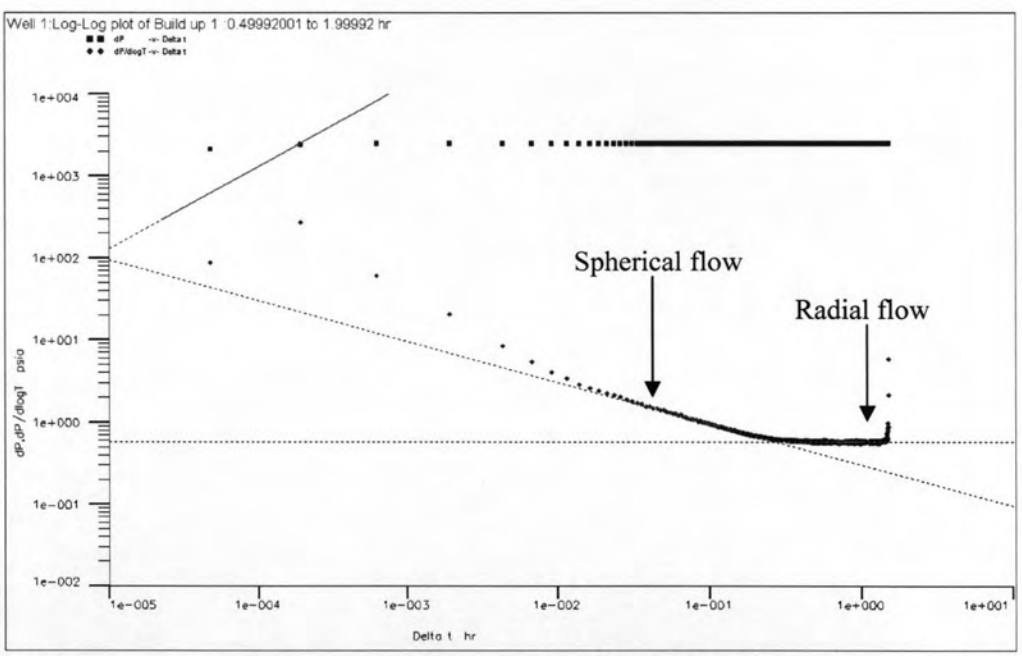

(b) Permeability anisotropy ratio of 0.05

Figure 5.10 : Diagnostic plots for different permeability anisotropy ratios.

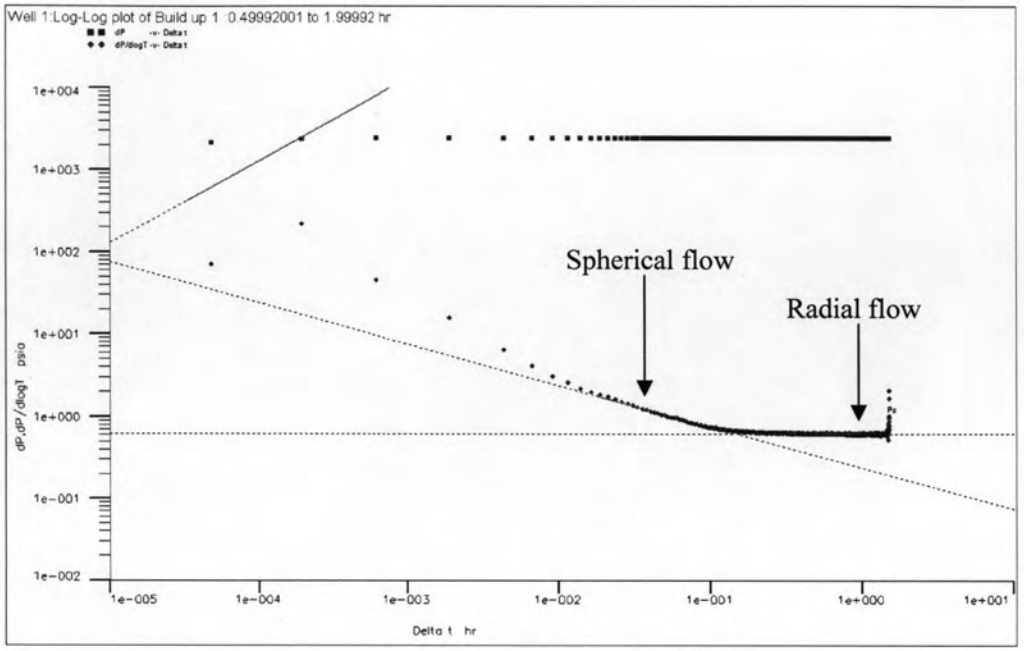

(c) Permeability anisotropy ratio of 0.1

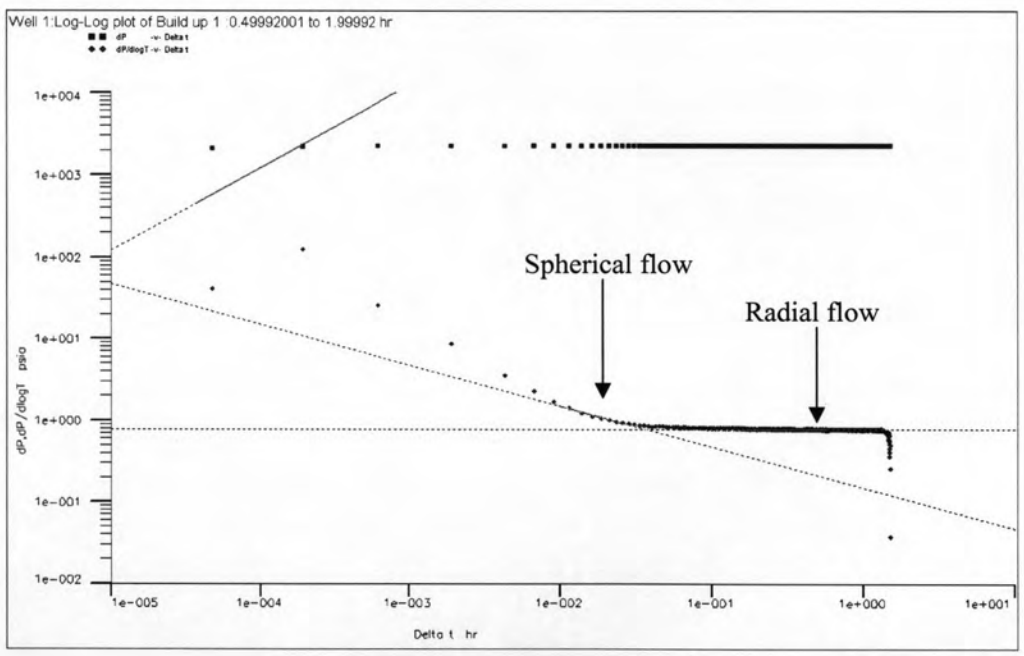

(d) Permeability anisotropy ratio of 0.5

Figure 5.10 : Diagnostic plots for different permeability anisotropy ratios (continued).

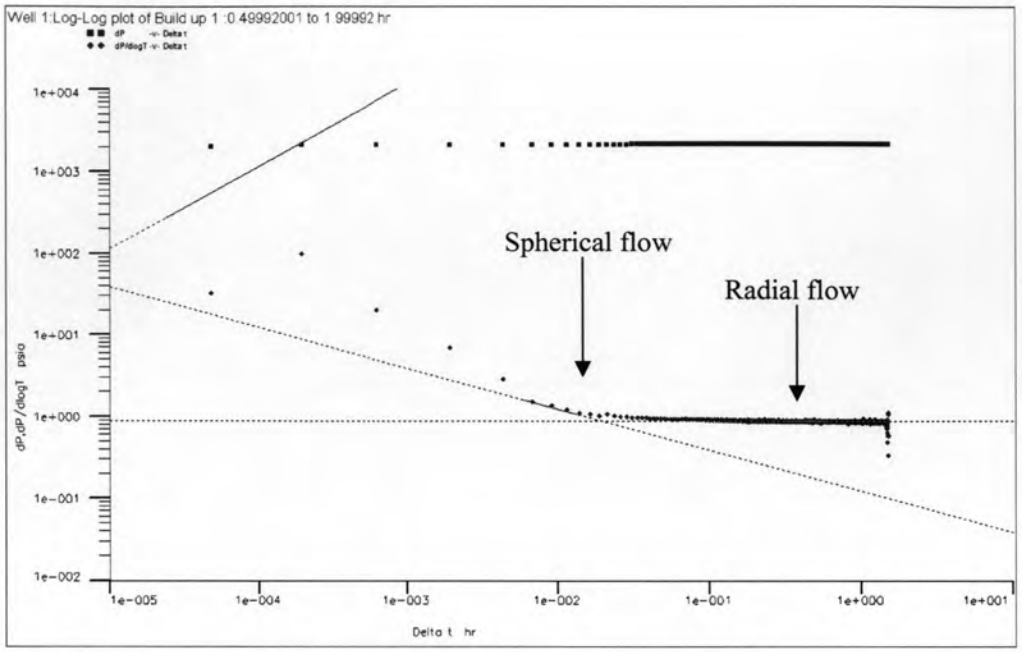

(e) Permeability anisotropy ratio of 1

Figure 5.10 : Diagnostic plots for different permeability anisotropy ratios (continued).

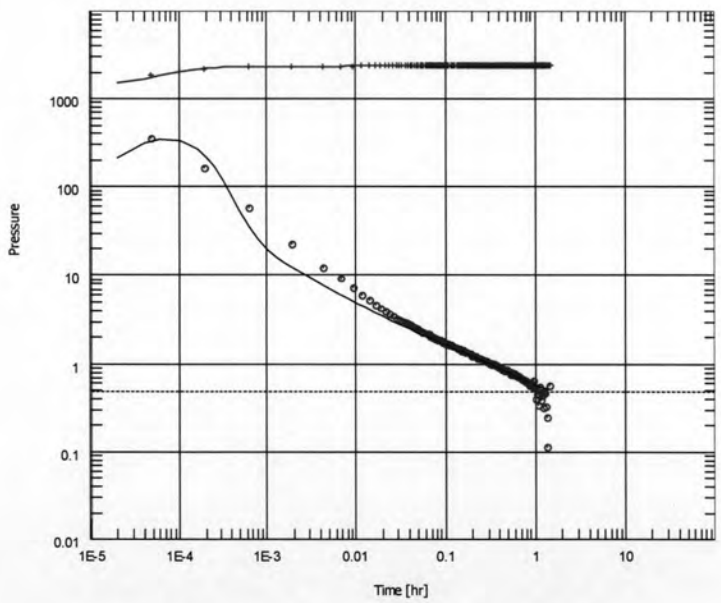

(a) Permeability anisotropy ratio of 0.01

Figure 5.11 : Regression plots for different permeability anisotropy ratios.

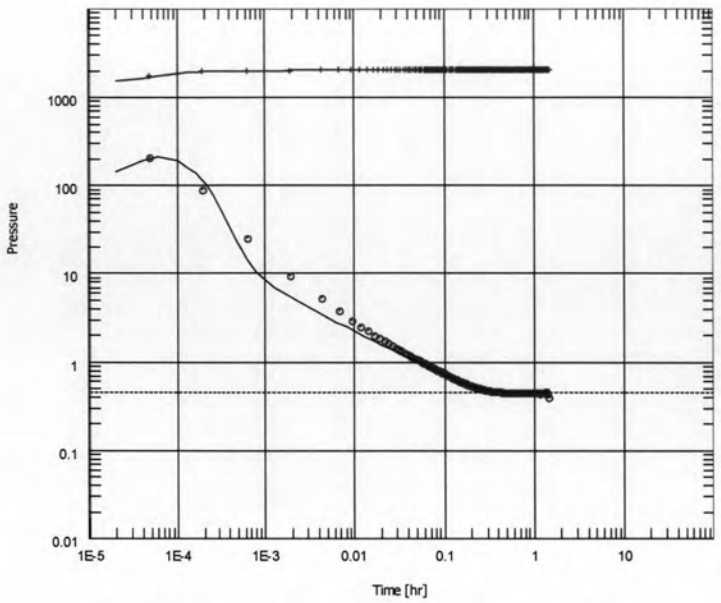

(b) Permeability anisotropy ratio of 0.05

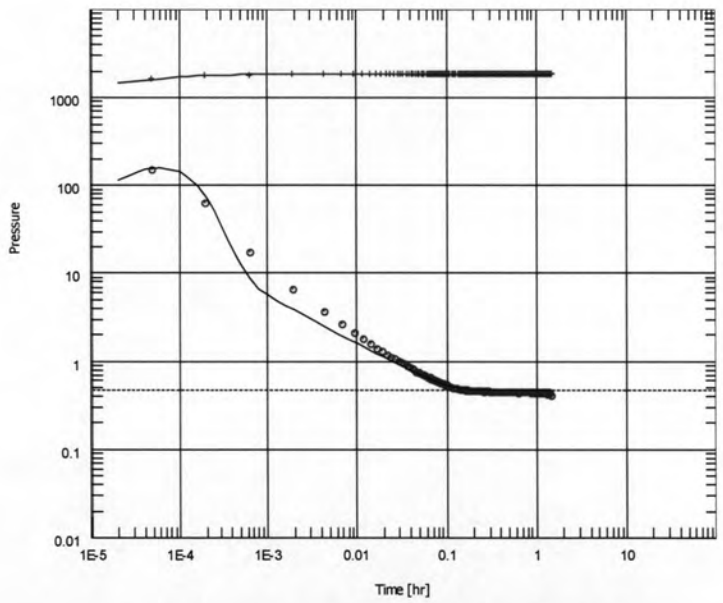

(c) Permeability anisotropy ratio of 0.1

Figure 5.11 : Regression plots for different permeability anisotropy ratios (continued).

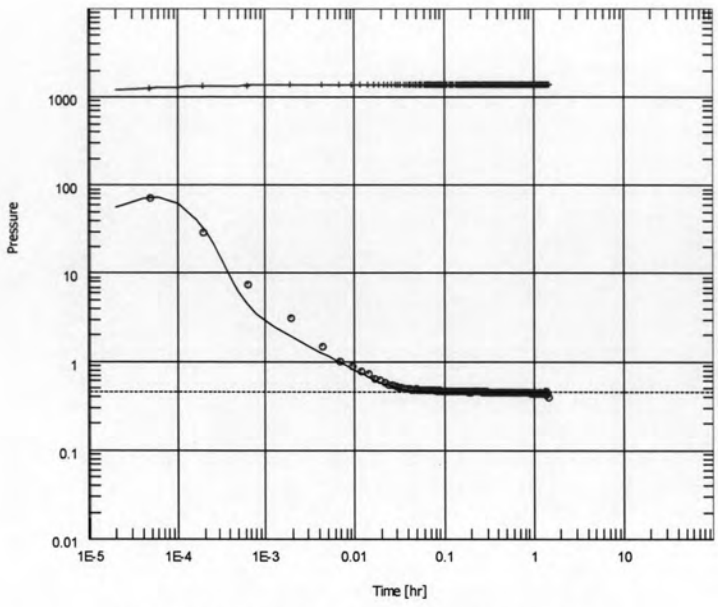

Log-Log plot: dp and dp' [psi] vs dt [hr]

(d) Permeability anisotropy ratio of 0.5

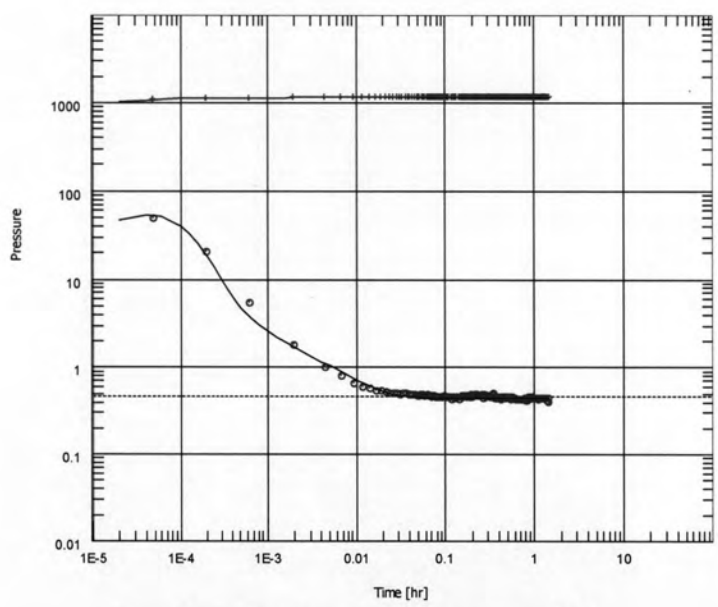

Log-Log plot: dp and dp' [psi] vs dt [hr]

(e) Permeability anisotropy ratio of 1

Figure 5.11 : Regression plots for different permeability anisotropy ratios (continued).

Table 5.3 : Interpreted results for different permeability anisotropy ratios.

Case	K_z/K_{xy}	K_z (mD)	Interpreted results (mD)		Error (%)	
			K_{xy}	K_z	K_{xy}	K_z
K10-1	0.01	0.1	8.385	0.1203	-16.15	20.3
K10-2	0.05	0.5	9.959	0.4760	-0.41	-4.8
K10-3	0.1	1	9.931	0.8949	-0.69	-10.51
K10-4	0.5	5	9.816	3.567	-1.84	-28.66
K10-5	1	10	9.864	6.684	-1.36	-33.16

From Figure 5.10, it can be seen that in the case of low permeability anisotropy ratio, the period of spherical flow regime is longer than that of high permeability anisotropy ratio. Therefore, in order to see the radial flow regime in very low permeability anisotropy reservoir such as in case K10-1, the test needs to be conducted for a longer period of time.

The interpreted results of this study are depicted in Table 5.3. In the case of permeability anisotropy ratio equal to 0.01 or case K10-1, the estimated horizontal permeability is different from the value used in the simulation (10 mD) with an error of -16.15 %. As can be seen in Figure 5.10 (a), the spherical flow period is long while the radial flow regime is still not fully developed at late times. The radial flow regime is needed in order to estimate the horizontal permeability. For this reason, the error from estimated horizontal permeability of this case is more than that of other cases.

In the case of high permeability anisotropy ratio such as cases K10-4 and K10-5, the error of estimated horizontal permeability is quite small but the error of the estimated vertical permeability are -28.66 and -33.16 % for case K10-4 and K10-5, respectively. These numbers are quite high. As can be seen in Figure 5.10 (d) and (e), the spherical flow period is small compared with other cases in Figure 5.10 (a), (b), and (c). The spherical flow regime is needed in order to estimate the vertical permeability. Because of the spherical flow regime is not clear enough, so the errors for these two cases are high compared with other cases. From Figure 5.11 (a), (b), (c), (d), and (e), the regression shows good matches to the data in the diagnostic plot.